Trade-off between Losses and EMI Issues in Three-Phase SiC Inverters for Aircraft Applications

Victor Dos Santos[1,2], Bernardo Cougo[1], Nicolas Roux[2], Bruno Sareni[2], Bertrand Revol[3], Jean-Pierre Carayon[1]
[1] IRT Saint Exupéry, 118 route de Narbonne, 31432 Toulouse cedex 4, France
Email : victor.dossantos@irt-saintexupery.com - bernardo.cogo@irt-saintexupery.com
[2] Université de Toulouse, LAPLACE, UMR CNRS-INP-UPS, 2 rue Charles Camichel, 31071 Toulouse cedex, France
Email: nicolas.roux@laplace.univ-tlse.fr - bruno.sareni@laplace.univ-tlse.fr
[3] SATIE – ENS Paris Saclay, PRES UniverSud 61 avenue du Président Wilson, 94235 Cachan cedex, France
Email: bertrand.revol@satie.ens-cachan.fr

***Abstract*—Power converters will only be effectively used in future aircrafts if they are compact, efficient and reliable. All these aspects can be improved by the use of disruptive technology such as the so-called Wide Bandgap (WBG) semiconductors made of Silicon Carbide (SiC) or Gallium Nitride (GaN). These components can switch much faster than their silicon counterpart, which can reduce converter losses and also decrease differential mode filter given the increase of switching frequency. However, such a fast commutation increases Electromagnetic Interference (EMI) issues in the converter and loads connected to it. This paper shows the approach developed at the French Institute of Technology (IRT) Saint-Exupery, in order to evaluate the trade-offs between losses and EMI issues of three-phase inverters used in future aircraft applications. Given the voltage DC bus of 540V, SiC MOSFETs are investigated and experimental results show the impact of these components on losses and EMI for different parameters.**

Keywords—Drive; Inverters; Wide Bandgap; SiC; EMI; EMC models; conducted emissions; common mode.

I. INTRODUCTION

The aircraft industry has been pushing toward the concept of More Electric Aircraft (MEA) to improve aircraft performance on one hand, while ensuring compliance to ACARE (Advisory Council for Aeronautics Research in Europe) environmental requirements for 2020 on the other hand. Aircraft operators expect cheaper, lighter and more reliable solutions. However, most projections show that with currently mature technologies, the full electrification of aircraft systems does not lead to significant enough mass savings. One of the main challenges associated to More Electric Aircraft is thus to drastically increase the power density of electrical power systems, without compromising on reliability.

As it can be seen in literature in the last few years, the development of new Wide Bandgap (WBG) semiconductor technologies (transistors and diodes), can significantly increase efficiency, performance and power density of adjustable speed electrical power drive systems. These components, made of Gallium Nitride (GaN) or Silicon Carbide (SiC) offer faster switching speeds, low losses, and the ability to operate at high temperatures compared to their silicon counterparts. Nevertheless, due to their higher switching speed (dv/dt) and voltage overshoot, WBG semiconductors used in power converters of an electromechanical chain may have some drawbacks when it comes to Electro-Magnetic Interference (EMI). Understanding the switching behavior of WBG components is necessary in order to keep switching speed and overvoltage at a reasonable level. Finally, one of the major challenges is to ensure that the introduction of this emerging technology does not lead to a regression of performance at system level.

In this paper, the characterization results of the SiC power module are described, first. Secondly, the common mode modeling of each part in the system is presented. Thirdly, some parametric studies are carried out to illustrate parameters influence on the trade-off between losses and common mode currents spectrum.

II. ELECTRICAL POWER DRIVE SYSTEM DESCRIPTION

Three-phase inverter is one of the most used power converter in a More Electrical Aircraft. Applications using this type of converter are electromechanical actuators, cabin pressurization system, oil/fuel pumps, engine starter and others. Another important application is the Integrated Modular Power Electronics Cabinet (IMPEC) concept, described in [1]. It consists of several power converters having the same characteristics which can be switched to supply several different loads inside an aircraft. Smart use of these modular power converters can reduce volume, weight and cost of electrical power systems in modern aircrafts.

One of the ideas [2] is to produce standard modular three-phase inverters having 45 kVA nominal power, at 540 V DC bus voltage and currents from 0 to 80 A per phase. The characteristics of this converter will be used as reference in this paper. One of first SiC MOSFET modules found in the market which could be used to cope with such power and voltage is the half bridge 1200 V/100 A SiC MOSFET module from CREE, reference CAS100H12AM1. The characterization of this SiC module will be performed in part 3 in order to show the trade-off between losses and EMI issues on three-phase inverters using SiC technology.

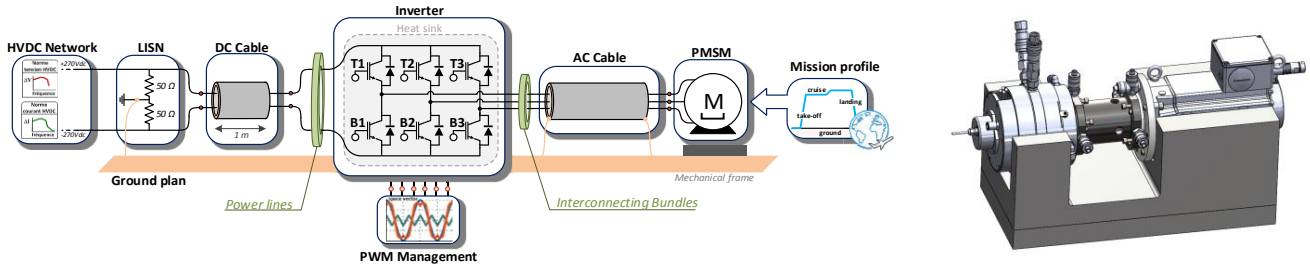

Fig. 1. Electromechanical Drive in the normative conditions according to the DO-160 Standard & Coupled electrical motors.

The studied system is a variable speed electrical power drive system. Fig 1 provides a schematic overview of the studied system. It is composed of two Line Impedance Stabilization Network (LISN), a three-phase SiC MOSFET inverter, an aeronautical Permanent Magnet Synchronous Motor (PMSM) and two non-shielded aeronautical cables (AWG 8 - Copper strands, insulation PTFE and Polyimide tapes): one links up the LSIN and the inverter (two conductors, one meter length) and another connects the inverter to the motor (three conductors, two meter length). Cables are the main elements to transport conducted EMI to the motor and other parts of the system. The electromechanical drive will be situated on a 6 m² copper plane, excluding a loaded induction generator used as the load of the system placed over insulation foams to insulate them from the ground. The complete system will be placed in a Faraday cage.

III. Characterization of SiC Power Module

A. Characterization Method

Calculation of semiconductor losses in three-phase inverters depends on conduction and switching losses. Conduction losses can be calculated using information provided by component's datasheet. Switching losses are not always possible to calculate using data sheet because either there is not enough data given by manufacturers or because they may not be representative of losses in the real converter.

Switching energies in datasheets are often measured using the "double pulse" method. This method has serious drawbacks including current sensing using resistors or a current transformer which changes the commutation loop resistance and the current in the transistor's parasitic capacitance which is not measured by this method. As a consequence, the calculated switching energy may be inaccurate, especially when it is applied to fast switches such as SiC transistors.

A more accurate method for measuring switching losses in fast components such as SiC and GaN transistors is called the "modified opposition method" and is explained in [3]. This method consists in an association of two identical half bridges containing the four identical devices (SiC MOSFETs in this case) supplied by the same source. One half-bridge operates as a generator and the other as a receptor. An inductive link connects both converters. The control of the current flowing from one half-bridge to the other is made by small differences applied to the duty cycle phase-shift of applied switching signals of both half-bridges. Like this, one can estimate turn-on and turn-off losses separately (Fig. 2). We applied this method in a test bench used for measurement of switching characteristics. A test board designed to characterize the CAS100H12M1 SiC module is presented in Fig. 3.

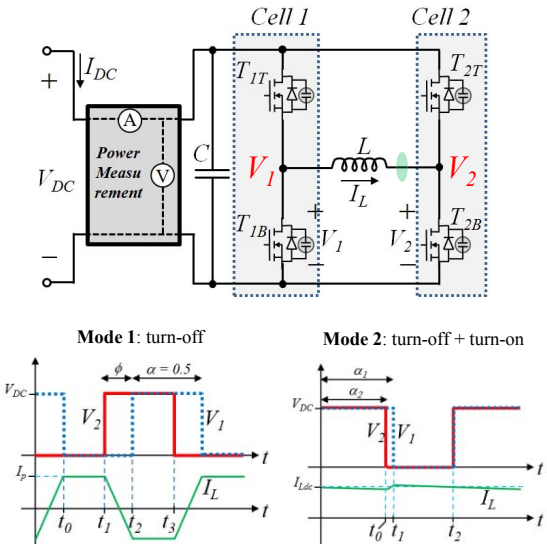

Fig. 2. Operating principle of the characterisation method.

As a result the variation of switching losses, switching speed (dv/dt) and also overshoot with circuit parameters (DC bus voltage V_{DC} and current I) and driver parameters (gate-source voltage V_{gs}, gate resistance Rg and dead time DT) are available from the module characterization.

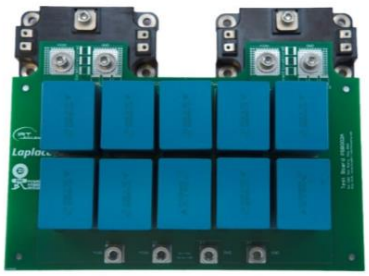

Fig. 3. Developed test board used for switching energy measurement specifically designed for the CAS100H12AM1 modules.

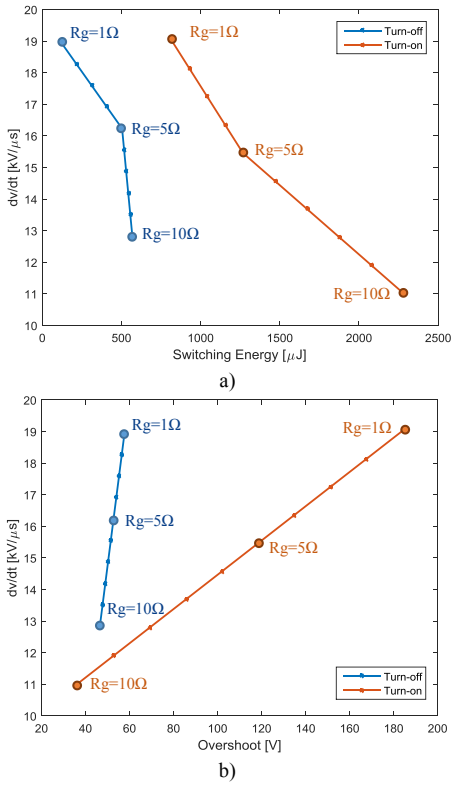

Fig. 4. Relationship switching speed and a) turn-on and turn-off energies and b) overshoot, for different *Rg*, at V_{DC} = 540 V and *Iout* = 50 A.

As an example of the experimental results described above, Fig. 4a shows the relationship between dv/dt and switching energies (turn-on and turn-off) and gate resistance at 50 A, for a DC bus voltage of 540 V and *Vgs*=20 V. The same is shown in Fig. 4b, but related to the overshoot.

These figures show the bigger the *Rg* is, the higher switching losses are, but the lower the overshoot and switching speed dv/dt are.

Note that, when changing *Rg* from 10 to 1 Ω, the total energy (turn-on + turn-off) decreases from around 2850 µJ to 930 µJ (3 times lower switching losses). However, the maximum dv/dt and maximum overshoot increase 1.5 and 4 times, respectively.

B. Losses, Switching Speed and Overshoot Results

Having the experimental data described above, one can evaluate losses of a three-phase inverter and associate it to dv/dt and overshoot values. This is done using a MATLAB algorithm to calculate transistors switching and conduction losses for different converter's switching frequencies and output current per phase. Three configurations are evaluated, including an IGBT for comparison purposes: 1 – using the Si IGBT SK100GB12T4 module (referred here as "IGBT Datasheet"); 2 – using the SiC module based on the previous characterizations having *Rg*=5 Ω and *Vgs*=20 V; 3 – using the same SiC module, based on the previous characterizations having *Rg*=1 Ω and *Vgs*=24 V. The last configuration is the one where one can reduce the most losses in the SiC module.

For the three different configurations, total losses are calculated for nominal power, i.e. for 80 A RMS current per phase and for two different switching frequencies F_{sw}, 15 kHz and 60 kHz. Calculation was made considering sinusoidal output currents in phase with the output voltage (i.e. resistive load), having negligible current ripple. Results of this calculation are shown in Table I.

TABLE I. LOSSES, SWITCHING SPEEDS AND OVERSHOOTS FOR DIFFERENT CONFIGURATIONS ON A 540V/45KVA/80A THREE-PHASE INVERTER USING SI IGBT OR SIC MOSFET

		Si IGBT Datasheet	***SiC R_g = 5 Ω***	***SiC R_g = 1 Ω***
Total Losses	F_{sw} = 15 kHz	423 W	450 W	357 W
	F_{sw} = 60 kHz	1323 W	828 W	507 W
Average Switching Speed		10 kV/µs	20 kV/µs	30 kV/µs
Max Overshoot		N/A	100 V	220 V

Besides the values concerning losses, we have added the average switching speed and the maximum overshoot for each configuration. They were calculated using experimental results for the SiC and using the datasheet values for the IGBT. Note that at low switching frequency (15 kHz), there are about 16 % lower losses when using SiC MOSFET (R_g = 1 Ω) compared to IGBT's. At high frequency (60 kHz), the fact of reducing the gate resistance from 5 to 1 Ω, and increasing the gate-source voltage, total losses of SiC module decrease almost 2 times. However this losses reduction increases dv/dt by 50% and doubles the maximum overshoot.

IV. CONDUCTED EMISSIONS MODELING

Knowing that conducted disturbances leads to premature damage in electrical motors, EMI must not exceed the permissible levels. When results are not compliant with the EMI standard, here the commercial aircraft standard DO-160 G, one or more passive EMI filters have to be added to efficiently reduce electromagnetic interference emissions. The study is especially focused on common-mode (CM) conducted noise emissions, which are the most disturbing in any variable-speed drive systems.

Conducted emissions modeling of such system is generally difficult because of it requires considering parasitic couplings in converters, feeding cables and motor windings. Consequently, a good expertise of all CM currents path is needed. Previous work has focused on creating models in a circuit type simulation environment. Results are obtained using time-based methods. However, to assess EMI standards compliance, simulated temporal signals have to be converted into spectral signals using fast Fourier transform (FFT) algorithm. Computing time of those time-based methods strongly depends on the smallest time constant of the system and on the maximum frequency desired. The modeling principle proposed here directly provides the results in the frequency domain. The idea is to represent the CM equivalent circuit as a chain of two-port networks corresponding to each component of the system. In this section, CM equivalent circuits and results from this interesting approach will be presented.

A. LISN Model

LISN is a device used in conducted emission tests, as specified in various EMC test standards. LISN are used to prevent incoming conducted emissions from the power supply and to maintain the stabilized impedance 50 Ω in a wide frequency range. The parameters of the LISN circuit topology are provided by the manufacturers. A simplified predictive CM model consists in a resistance and a capacitor connected in series ($R_0/2$, $2.C_0$), where $R_0 = 50\ \Omega$ and $C_0 = 0.2\ \mu F$.

B. Inveter Model

A well-known practice to represent the switching voltage is to simply model it by a trapezoidal waveform. The idea here is to increase the accuracy of this waveform by adding the information of dv/dt and overshoot experimentally obtained. Data shown in Table 1 are not sufficient to preview EMI issues in converters. For this, dv/dt and overshoot must be known for each commutation of an entire period of the output current. Thus, an algorithm was developed to calculate dv/dt and overshoot of each switching period based on experimental results (Fig. 5 and Fig. 6).

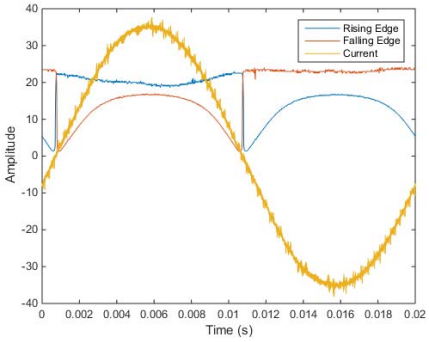

Fig. 5. Switching speed [kV/µs] during one output current period.

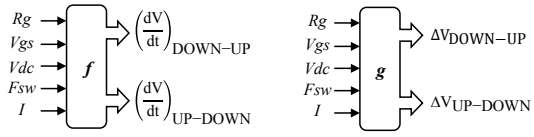

Fig. 6. Linear interpolations functions (f, g) for switching speed and overvoltage calculation.

This type of waveform can be mathematically described as a function of the form $K.e^{-\alpha.t}.\sin(\omega_r.t)$, where α is a damping coefficient and ω_r is the pulsation of the ringing. These two parameters are issued from experimental data; they are mainly dependent on the circuit parasitic inductance, capacitance and resistance and do not significantly change with the driver parameters and output current. This ringing tends to accentuate or enhance certain regions of the spectrum of the original waveform. Undershoot and overshoot have the effect of increasing the emissions about the ringing frequency.

As a result, the trapezoidal waveform is modified as shown in Fig 7 which is a much better representation of an actual experimental waveform.

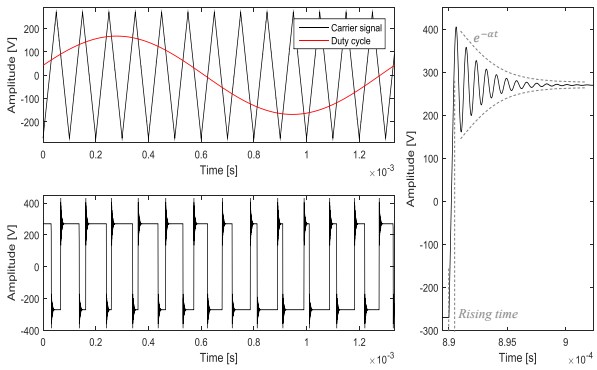

Fig. 7. Mathematical generation of output phase voltage waveform.

In this approach, the CM noise source is represented by the CM voltage regarding the load, which can be defined as done in equation by

$$V_{CM} = (V_{U0}+V_{V0}+V_{W0})/3 \quad (1)$$

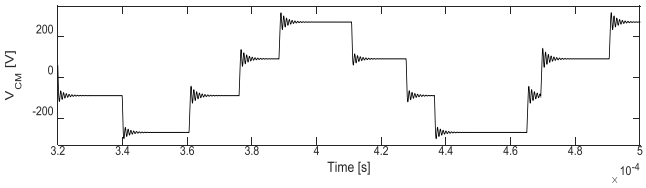

Fig. 8. Analytical CM Voltage waveform.

The three legs of the inverter, generating V_{CM}, can be considered as a single perfect voltage source, as represented in Fig.8. All parasitic CM capacitances are identified as follow. The values of C_{i0} and C_{o0} are determined using an impedance meter with, respectively, the busbar, the three legs short-circuited. The measured impedance is mainly capacitive until 100 MHz; therefore, C_{o0} is assimilated to a capacitance equal to 2.8 nF.

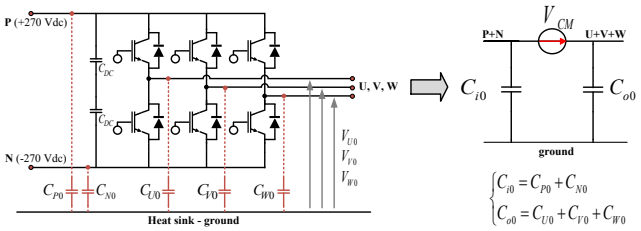

Fig. 9. Equivalent circuit of the inverter (CM point of view).

C. Cable Model

AC cables can be viewed as a three conductor transmission line guided by transmission line theory [4]. The method used to determine the cable parameters consists in using an electromagnetic solver tool. This method makes it possible to extract the inductance, resistance and capacitance between the power cable conductors. In this study, the finite element code "FEMM software" was used. All conductors are in parallel and the AC cable CM model can be described as in Fig. 10.

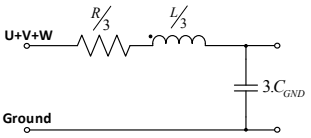

Fig. 10. CM equivalent circuit of the AC Cable.

In order to increase the representativeness of those cables models, frequency dependency has to be taken into account, due to skin and proximity effects (Fig. 11, Fig. 12) and the dielectric losses in the cable.

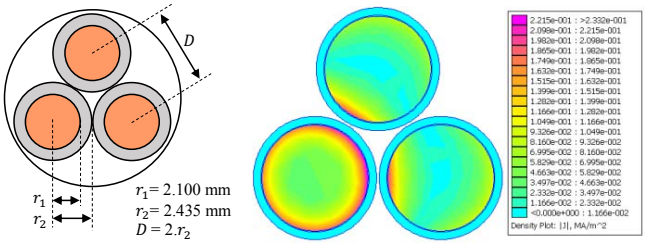

Fig. 11. Geometrical parameters and current density plot at f = 20 kHz.

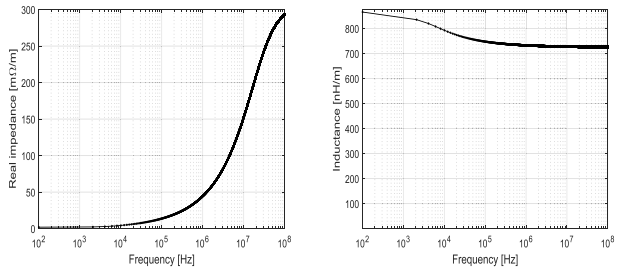

Fig. 12. Evolution of the resistance and inductance depending on frequency.

The same reasoning also applies to the case of a two conductor transmission line for the DC cable.

D. Motor Model

The electrical machine is a main propagation path for CM conducted emission of the drive system. Vector fitting method is proposed to model the PMSM, using measured impedance data. The vector fitting method has been introduced since 1999 by Gustavsen and Semlyem [5] and is widely used for fitting a rational function for frequency domain response.

[6] By applying vector fitting, the rational function of the CM motor impedance, obtained by experimental data, can be approximated by a transfer function *h(s)* as

$$h(s) \approx d + s.e + \sum_{k=1}^{n} \frac{r_k}{s - p_k} \qquad (2)$$

where r_k and p_k are the *k*th residue and pole of the formula. Respectively, they could be real or complex conjugate pairs while *d* and *e* are real. If it is an impedance application as used in this paper, *s* is equivalent to $j\omega$ where ω is the angular frequency.

This transfer function can be divided into several sub-circuits in terms of order of the function as shown in Table II.

TABLE II. TYPICAL TRANSFER FUNCTIONS AND EQUIVALENT CIRCUITS

Transfer functions	d	$e.s$	$\frac{r}{s-p}$	$\frac{r_1}{s-p_1}+\frac{r_2}{s-p_2}$
Equivalent circuits				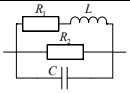

The CM impedance is obtained by using an impedance analyzer in the frequency range from 1 kHz to 100 MHz.

In consideration of a trade-off between the accuracy and the complexity of the equivalent circuit by using a vector fitting method, 4-order approximation is used to model the CM impedance of the motor winding with a corresponding circuit topology shown in Fig. 13.

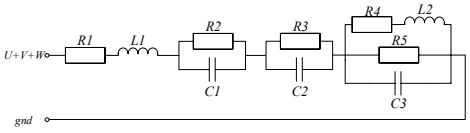

Fig. 13. Equivalent circuit of the electrical motor CM impedance.

An optimization routine has been developed in order to evaluate the equivalent circuit parameters values. The quasi-Newton algorithm to minimize an error criterion in (3) is used.

$$\varepsilon = \sum_{f_i=f_0}^{f_n} f_i \left| Z_{CM-MEAS}(f_i) - Z_{CM-FIT}(f_i) \right|^2 \qquad (3)$$

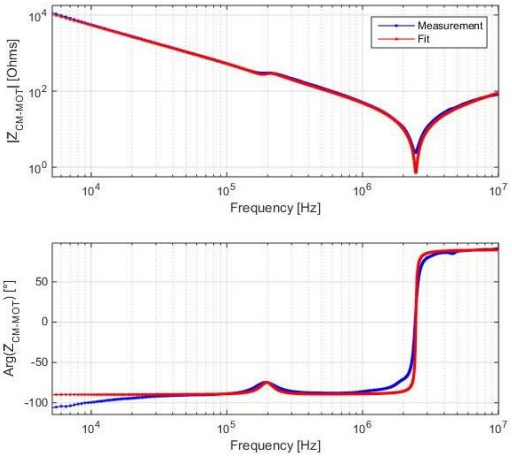

Fig. 14. Measurement and simulation results for motor CM model.

The simulated and experimental results of CM impedance are shown in Fig. 14. The comparisons of magnitude and phase data show that the simulation results of 4-order equivalent circuit matches the experimental results well in the entire bandwidth.

E. Quadripolar Approach

As previously mentioned, the model is represented by a chain of two-port networks characterized by an impedance matrix [Z], as shown in Fig. 15, which is then transformed into a transfer matrix [T] in order to easily compute the equivalent matrix of the consecutive two-port networks in cascade. The coefficients of matrix [*Z*] are defined in (4).

$$[Z]=\begin{bmatrix} Z_{11}=V_1/I_1)_{I_2=0} & Z_{12}=V_1/I_2)_{I_1=0} \\ Z_{21}=V_2/I_1)_{I_2=0} & Z_{22}=V_2/I_2)_{I_1=0} \end{bmatrix} \quad (4)$$

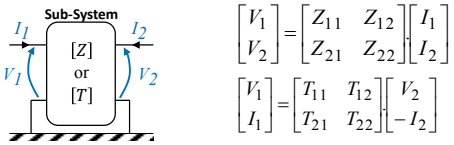

$$\begin{bmatrix} V_1 \\ V_2 \end{bmatrix}=\begin{bmatrix} Z_{11} & Z_{12} \\ Z_{21} & Z_{22} \end{bmatrix}\begin{bmatrix} I_1 \\ I_2 \end{bmatrix}$$

$$\begin{bmatrix} V_1 \\ I_1 \end{bmatrix}=\begin{bmatrix} T_{11} & T_{12} \\ T_{21} & T_{22} \end{bmatrix}\begin{bmatrix} V_2 \\ -I_2 \end{bmatrix}$$

Fig. 15. Two port networks representation.

The relation between the matrices [T] and [Z] is defined by

$$[T]=\begin{bmatrix} T_{11}=Z_{11}/Z_{21} & T_{12}=(Z_{11}.Z_{22})/Z_{21}-Z_{12} \\ T_{21}=1/Z_{21} & T_{22}=Z_{22}/Z_{21} \end{bmatrix} \quad (5)$$

When any two port networks are associated, the equivalent matrix $[T_{eq}]$ is obtained simply by carrying out the matrix multiplication of the two initial matrices.

Previous studies underline the fact that transfer of mode, differential mode to common mode, may exist especially if there is a dissymmetry of component structure at CM point of view. As a first approximation for the CM currents calculation, we consider the harmonic content of the differential mode current negligible due to the filtering effect of the cable and of the motor inductances. This is why, the modeling principle is based on the hypothesis that the CM currents are mainly due to the CM voltage, as carried out in [7]. The electromechanical drive can be modeled with a quadripolar approach as shown in Fig. 16.

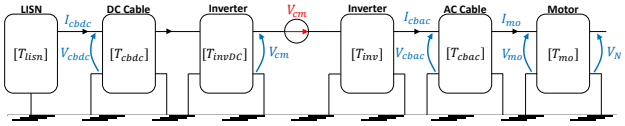

Fig. 16. Common mode quadripolar chain.

This mathematical approach allows to easily to take account of the frequency dependency of each matrix. Results are obtained in less than 300 ms and shown in Fig. 17. As expected, the gate resistance affects the frequency band between 7 MHz to 30 MHz. This is important to consider the continual increase to high frequencies issues in more electrical aircraft applications. Therefore, models have to be robust and valid in a large bandwidth from 100 kHz to, at least, 50 MHz for this new emerging technology.

V. Conclusion

The use of SiC components in three-phase inverters was investigated in this paper. The advantages of reducing losses due to fast commutation are quantified experimentally for the variation of different circuit and driver parameters. The disadvantage of such fast commutation on Electromagnetic Interference (EMI) issues. A generic approach to evaluate the trade-offs between losses is presented and EMI issues of three-phase inverters which is accurate and suitable for fast switches such as SiC and GaN transistors. Some results show that, reducing the gate resistance from 10 to 1 Ω, a SiC inverter may present three times lower switching losses although the maximum dv/dt of the output voltage increases 50% and larger high-frequency CM filters are necessary to filter an extra 10 dB at 14 MHz of the output CM current. In future works, this approach will be used efficiently to optimize EMI filters and mass repartition in the electromechanical chain, we will reason at operating system level. In order to achieve good electrical performance and EMI standard compliance, trade-offs between losses and EMI generation have to be found.

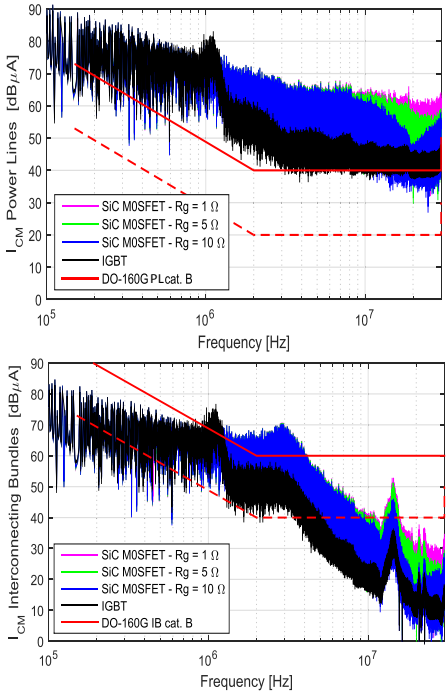

Fig. 17. CM currents at inverter input and output (F_{sw} = 15 kHz, *Iout* = 20 A).

References

[1] L. Prisse, D. Ferer, H. Foch, A. Lacoste, "New power centre and power electronics sharing in aircraft", 13th European Conference on Power Electronics and Applications (EPE), Barcelone, Spain. Sept. 2009.

[2] X. Giraud, M. Budinger, X. Roboam, H. Piquet, M. Sartor, J. Faucher, "Optimal desing of the integrated modular power electronics cabinet", Aerospace Science and Tecnhology, vol. 48, pp. 37–52, 2016.

[3] B. Cougo, H. Schneider, T. Meynard, Accurate switching energy estimation of wide bandgap devices used in converters for aircraft applications, (2013) 15th European Conference on Power Electronics and Applications (EPE), Sept. 2013.

[4] P. Clayton R. "Analysis of multiconductor transmission lines." John Wiley & Sons, 2008.

[5] B. Gustavsen, A. Semlyen. "Rational approximation of frequency domain responses by vector fittingn" IEEE Transactions on power delivery, 1999, vol. 14, no3, p. 1052-1061.

[6] K. Jia, G. Bohlin, M. Enohnyaket, R. Thottappillil. "Modelling an AC motor with high accuracy in a wide frequency range". IET Electric Power Applications, 2013, vol. 7, no 2, p. 116-122.

[7] C. Jettanasen, F. Costa, et C. Vollaire. "Common-mode emissions measurements and simulation in variable-speed drive systems". IEEE Transactions on Power Electronics, 2009, vol. 24, no 11, p. 2456-2464.